Bulletin of Electrochemistry 17 (10) October 2001, pp 449-458 0256-1654/2001/$ 3-50

ELECTROCHEMICAL BEHAVIOUR OF Al-Si ALLOYS IN ACID AND ALKALINE MEDIA

A A MAZHAR*, S T ARAB AND E A NOOR

Chemistry Dept, Girls' College of Edn, P O Box 9470. Jeddah 21413. KINGDOM OF SAUDI ARABIA
** Chemistry Department, Faculty of Science, Cairo University, Giza. EGYPT*

[Received: 29 September 2000 Accepted: 17 July 2001]

This study compares the electrochemical behaviour of three aluminium-silicon alloys in acidic and alkaline media by employing chemical, polarization and electrochemical impedance spectroscopy measurements in addition to scanning electron micrography. In general, aluminium-silicon alloys corrode at a rate higher than pure aluminium in these media. The corrosivity of the media was in the order of NaOH > H_3PO_4 > oxalic acid > H_2SO_4 > tartaric acid > succinic acid. The corrosion susceptibility of the alloys decreased in any of the study media as follows: Al - 11%, Si > Al - 7% Si > Al - 22% Si. The results were discussed taking into account the microstructural features of the alloys. While capacitive control was observed in H_2SO_4, resistive control was apparent in NaOH medium.

Keywords: Aluminium silicon alloys, corrosion, impedance, polarization, acid and alkaline media.

INTRODUCTION

Aluminium alloys have been recognized as excellent fuel materials for electrical power production [1]. While alloying improves the mechanical strength of aluminium, it can degrade the surface resistance or passivity. However, corrosion rates can be significantly lowered by choice of the proper alloy. Aluminium in solution exhibits significant resistance to corrosion because of the formation of a passive oxide layer. However, in the passive region pitting corrosion may occur, especially when chloride ions are present. In water, aluminium is covered by an oxide film, whose stability is well established between pH 4 to 8.5 [2-3].

Corrosion of aluminium alloys is often closely related to the type, amount and properties of intermetallic phases present in the matrix. Aluminium silicon is a simple eutectic system, the composition of the eutectic is 12.2 ± 0.1 at % Si. The solidification structures depend on many factors, the most important is the cooling rate [4]. Aluminium-silicon alloys are among the most important commercial alloys, especially where high pressure endurance is required.

The corrosion and pitting rates of aluminium alloys in aqueous solutions are dependent upon the concentration and type of anions present [5-7]. Anions participate in metal dissolution by formation of metal-anion species at the interface which aid metal dissolution when unstable and hinder further dissolution when stable [8].

The pH of zero charge for aluminium oxide is 9 to 9.1 [9]. The surface will be positively charged at pH < 9 and aggressive anions are likely to be adsorbed. While chloride ions attack the aluminium electrode surface [10], sulphate ions are non-aggressive as established by studies indicating the passivating character of H_2SO_4 [11]. In strongly alkaline solutions, OH^- dissolves the protective oxide film and the aluminium metal surface establishes a very negative potential, with formation of aluminate ions [12].

Studies on the electrochemical behaviour of aluminium-silicon alloys [13] are somewhat scarce. It is the purpose of this work to elucidate the role of some anions on the corrosion of aluminium alloys containing different additions of silicon and the degree of attack in the media under study.

EXPERIMENTAL

The composition of the three aluminium-silicon alloys and commercially pure aluminium used in the study is given in Table I.

TABLE I: Composition of Aluminium-silicon alloys and pure aluminium

Sample	Si	Cu	Zn	Pb	Co	Ni	Fe	Cr	Al
Al 7 % Si	7.0	0.048	0.004	0.001	< 0.02	0.023	0.163	0.006	Remainder
Al 11% Si	11.0	0.123	0.014	0.002	< 0.05	0.073	0.113	0.025	Remainder
Al 22% Si	22.0	0.282	0.021	0.007	< 0.05	0.385	0.179	0.056	Remainder
Pure Al	—	0.002	0.003	0.100	< 0.05	0.011	0.179	0.082	Remainder

All chemicals used were AR grade (BDH) except HCl (Fluka) and oxalic acid (Merck). Deionized water was used in the preparation of the solutions and for washing. Samples used in chemical measurements were in the form of rods 5 cm long and 1 cm in diameter. Electrodes used in polarization or electrochemical impedance spectroscopy, EIS, measurements were in the form of rods, embedded in glass tubes and fixed by Araldite adhesive (Ciba product, Switzerland). The reference electrode was Ag/AgCl. The auxiliary electrode was a Pt sheet. Before immersion in the test solution the surface was mechanically polished using finer grades of emery papers upto 4/0 and then washed with deionized water. For polarization measurements, solutions were deaerated with 99.999% pure nitrogen gas. The temperature was adjusted by using an ultra thermostat (Julabo U3 No. 8311) at 303 ± 2 K.

Potentiostatic polarization was conducted by an AMEL potentiostat (Model 533, Italy) with positive feed back for IR drop compensation. Electrochemical impedance spectroscopy (EIS) was carried out by the use of an impedance spectrum analyzer (Thales IM6, Germany) connected to a Samsung computer (Sync Master 15 GLi). All experiments were in the frequency range 100 KHz to 0.1 Hz. The input signal amplitude was 10 mV peak to peak in both high and low frequency ranges. Scanning electron microscopy (SEM) was employed to study the surface morphology by JEOL/JSM (T20 Japan) scanning electron microscope. The samples were studied after etching or 90 minutes immersion in the test solutions, in both cases after mechanical polishing.

RESULTS AND DISCUSSIONS

Fig. 1 shows the microstructural features of the alloy surfaces as well as pure aluminium. Al-11% Si is observed in the form of eutectic dendrites. Al - 7% Si contains aluminium grains surrounded by the eutectic and Al - 22% Si contains primary Si (H shaped) surrounded by the eutectic. Aluminium grains are observed in case of the pure aluminium sample.

The results of potentiostatic polarization, EIS and chemical measurements will be discussed in the following for each of the studied media.

H_2SO_4 medium

Polarization was conducted after immersion of the electrodes in the test solution till stable potential, open circuit potential (OCP) was reached. The electrodes were polarized in the anodic or cathodic direction starting from OCP. The sweep rate was 2 mVs^{-1}.

Polarization curves for the three alloys as function of H_2SO_4 concentration are shown in Fig. 2. On anodic polarization, the curves exhibit an active region which reaches limiting currents, i_1. The values of i_1 are proportional to acid concentration. This is a result of film thickening with increasing polarization which leads to a constant electric field and slow transport of the acid molecules [14]. At these potential regions, the process is thus diffusion controlled. Some anions, among which is sulphate and oxalate, allow some anodic dissolution resulting in formation of porous oxide layers of significant thickness and rather regular structure [15]. The shift in the current at which i_1 is attained to higher values with increase in acid concentration is attributed to attack of the film by the acid.

On cathodic polarization there is a shift to higher current densities with increase in acid concentration. This is followed by a shift in the opposite direction at higher concentrations, for

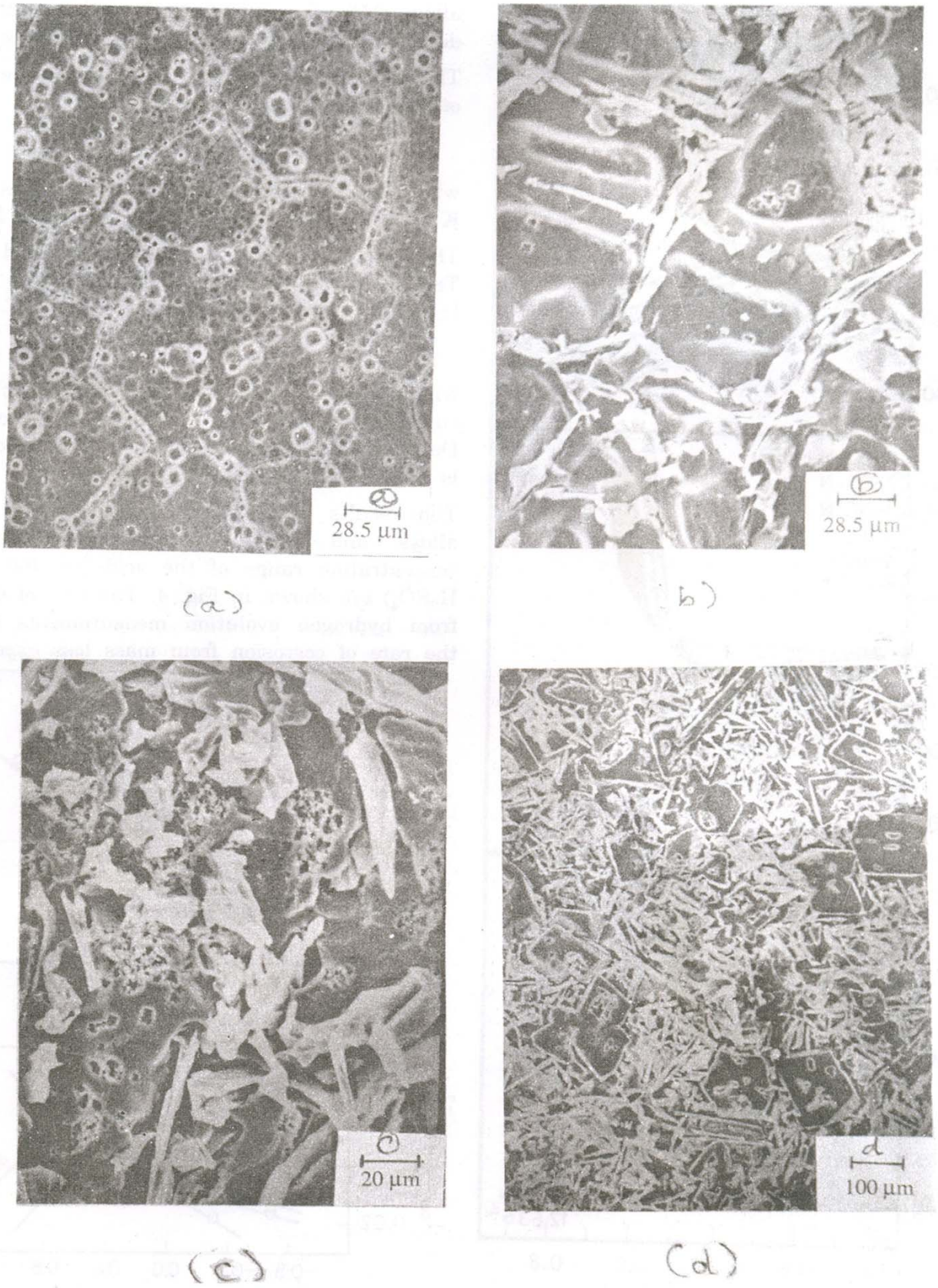

Fig.1: Micrographs for the etched samples
(a) pure Al: showing Al grains attacked by the etchent (b) alloy 7% Si: Al grains surrounded by acicular eutectic
(c) alloy 11% Si: structure is completely formed of the eutectic with very fine Al grains
(d) alloy 22% Si: primary Si surrounded by acicular eutectic

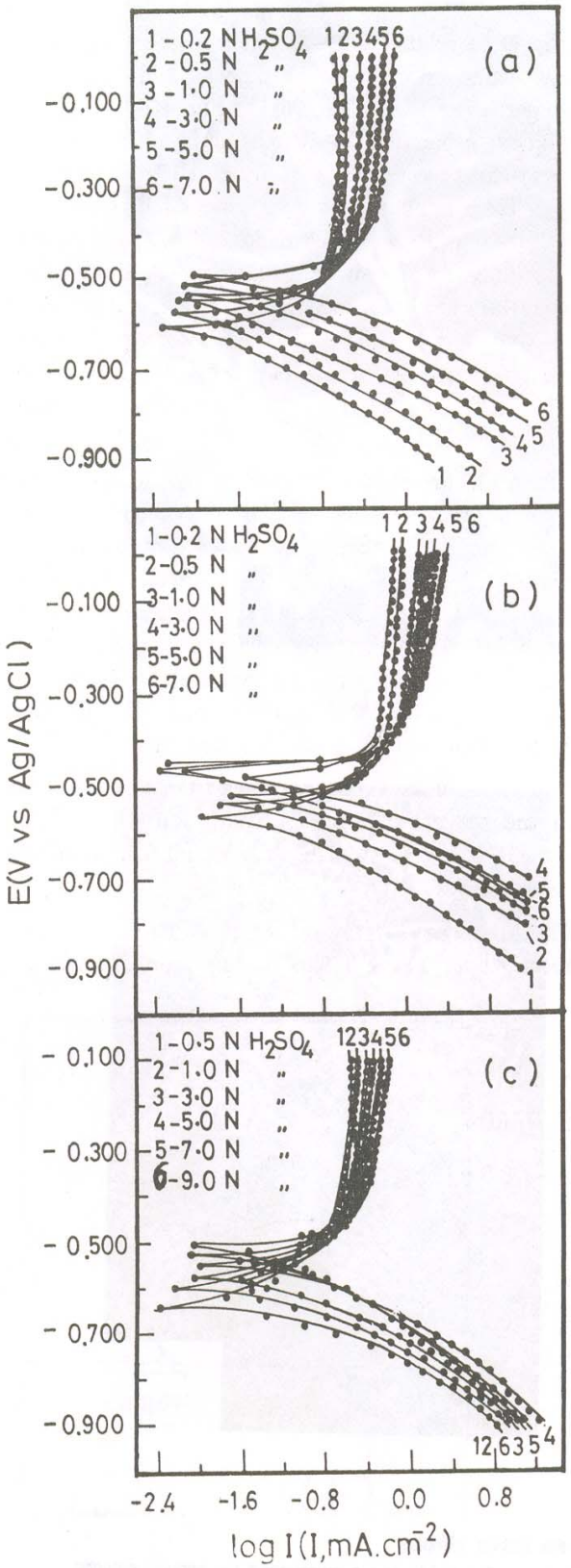

Fig. 2: Polarization curves as function of H_2SO_4 concentration for the alloys (a) 7% Si, (b) 11% Si and (c) 22% Si

alloys 11% Si and 22% Si which indicates a decrease in the rate of the cathodic process.

The dependence of OCP, E_0 on the concentration of the acid, c is represented by

$$E_0 = E_0^0 + K \log c \quad (1)$$

where E_0^0 is the value of E_0 at unit concentration, K is a constant dependent on the alloy, Fig. 3a.

The corrosion current, i_{corr} was obtained by the Tafel extrapolation. The relation between i_{corr} and log c, Fig. 3b is represented by:

$$i_{corr} = a + b \log c \quad (2)$$

where a and b are constants dependent on the characteristic of the corroding surface [16]. Decrease in i_{corr} values after the inflection point is attributed to oxide film growth.

The results of chemical measurements for the alloys and pure aluminium in the same concentration range of the acid (i.e. 0.5 to 9 N H_2SO_4) are shown in Fig. 4. The rate of corrosion from hydrogen evolution measurements (R) and the rate of corrosion from mass loss experiments

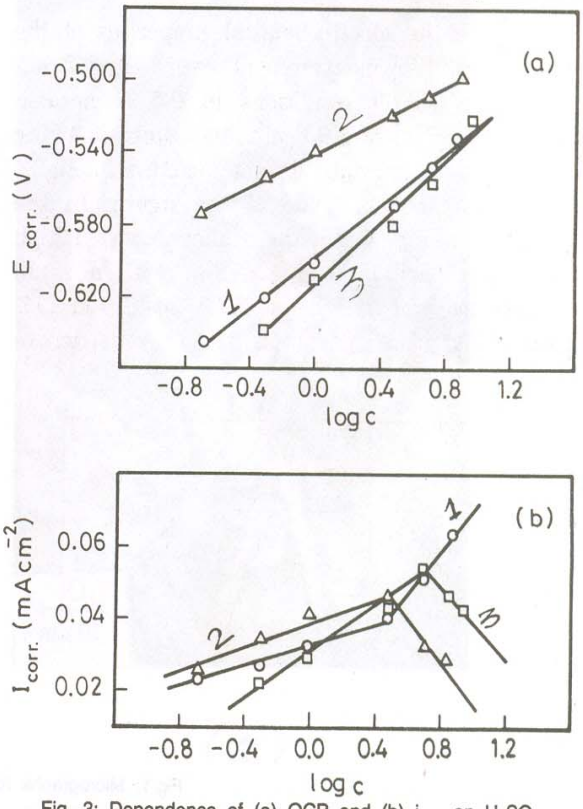

Fig. 3: Dependence of (a) OCP and (b) i_{corr} on H_2SO_4 concentration for the three alloys
(1) 7% Si, (2) 11% Si and (3) 22% Si

(R') were determined for each specimen in the concentration range under study. Values of both R and R' increase with increase in concentration for 7% Si, while 11% Si and 22% Si reach critical values after which both R and R' decrease with concentration. The highest values obtained for R and R' correspond to the same concentration at which the highest i_{corr} value was recorded for each alloy.

The decrease in i_{corr}, R and R' at high H_2SO_4 concentrations is explained by the fact that low concentrations of sulphate ions catalyze the HER, while at higher concentrations inhibition sets in due to the presence of the inner highly resistive layer which is not hydrated appreciably by sulphate ions [17]. The primary process in electrochemical corrosion of aluminium at pH ≤ 3 is the formation of $[Al\ (H_2O)_6]^{3+}$ [18]. It has been reported that increase in concentration of SO_4^{2-} suppresses the chemical dissolution in aluminium in H_2SO_4 containing sulphate salts, the surface becoming more even and the porosity near the outer surface reduced [19].

To compare the electrochemical properties of the three alloys, EIS measurements were carried out under open circuit conditions in 0.5 N aerated H_2SO_4 solutions after 60 minutes immersion. The plot for pure aluminium is not included in Fig. 5 since it was out of scale of the figure. In the Nyquist plot, Fig. 5 the three alloys show a high frequency capacitive loop, together with a small inductive loop for 7% Si (at 697.8 mHz) and 11% Si (at 365.2 mHz). The high frequency capacitive loop is correlated with the dielectric properties of the oxide film, i.e. thickness and dielectric properties of the barrier oxide film [20]. The well defined capacitive semicircle suggests that the corrosion process occurs under activation control [6]. The inductive loop is correlated with the localized process of corrosion. The polarization resistance, R_p can be determined from the diameters of the semicircles. It is highest for 22% Si and lowest for 11% Si, as observed from polarization measurements. The semicircles are depressed below the axis due to surface inhomogenities [20].

The oxide layer on aluminium alloys is viewed as both a primary resistor and a dielectric of the condenser [21]. From the Bode plot shown in Fig. 6 the capacitance of the oxide layer is determined from $C = 1/2\ \pi f R_p$ where f is the frequency at which the imaginary part of the impedance lay at the maximum at f = 0.16 Hz (or log ω = log 2πf = zero) and R_p is the polarization resistance at this frequency.

The value of the impedance, z at f = 0.16 Hz was in the order 0.942, 1.199, 1.831 and 4.17 K Ω for 11% Si, 7% Si, 22% Si and pure aluminium respectively.

The highest value for the capacitance C was that recorded for 11% Si. This is due approximately to

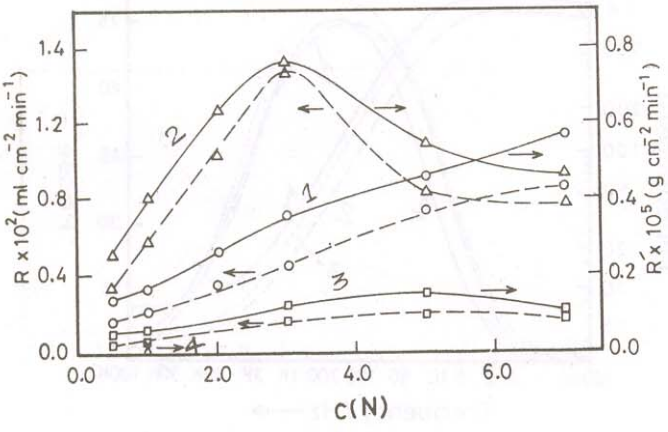

Fig. 4: Dependence of R and R' on H_2SO_4 concentration for three electordes.
(1) 7% Si (2) 11% Si (3) 22% Si (4) Pure aluminium

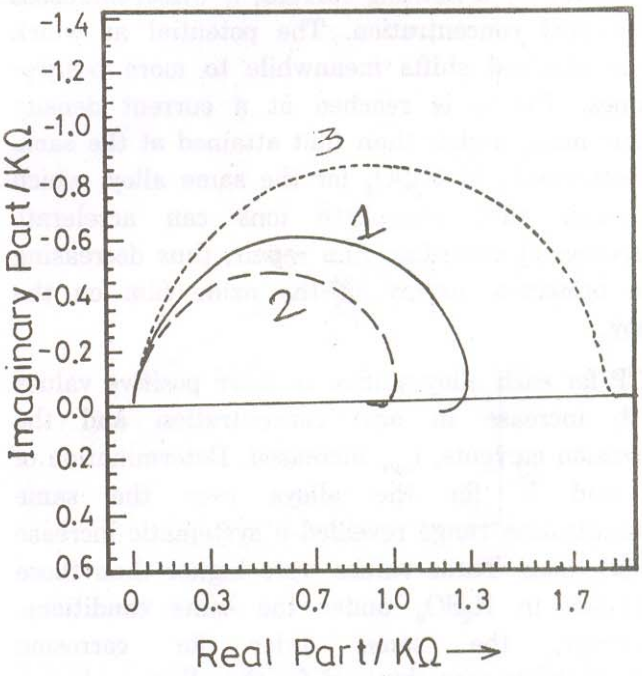

Fig. 5: Nyquist plot for the three alloys in 0.5 N H_2SO_4
(1) 7% Si (2) 11% Si (3) 22% Si

decrease in the effective thickness of the oxide layer, since the capacitance of a dielectric medium is given by [21].

$$C = k\,\varepsilon_0\,\frac{A}{\sigma} \qquad (3)$$

where K is the dielectric constant of the oxide layer, ε_0 is permittivity of free space (8.8×10^{-4} F cm^{-1}) [22]. A and σ are the area and thickness of the oxide layer, respectively.

The impedance in the medium frequency range in the Bode plot is determined by the capacitance C and for a pure capacitive behaviour the slope of log Z vs log f should be equal to -1 and θ rising towards 90^0 which is observed in the present case in H_2SO_4. Values of θ_{max} are in the order 22% Si > 7% Si > 11% Si, in agreement with polarization and chemical measurements which indicated that 22% Si has the best electrochemical properties among the three alloys. Values of R_p are in the same order as θ_{max}.

H_3PO_4 medium

Polarization measurements for the three alloys were conducted in H_3PO_4 solutions in the concentration range 3×10^{-2} to 3 N. For all alloys, increase in concentration leads to a systematic shift of both the cathodic and anodic branches to higher current density values. The anodic branch is limited by a limiting current, i_1 which increases with acid concentration. The potential at which i_1 is attained shifts meanwhile to more positive values. The i_1 is reached at a current density value much higher than that attained at the same concentration in H_2SO_4 for the same alloy, which indicates that phosphate ions can accelerate corrosion by retarding film repair, thus decreasing the protective nature of the oxide film on the alloy.

OCP for each alloy shifted to more positive values with increase in acid concentration and the corrosion currents, i_{corr} increased. Determination of R and R' for the alloys over the same concentration range revealed a systematic increase in all cases. These values were higher than those obtained in H_2SO_4 under the same conditions. However, the same order for corrosion susceptability was obtained for the alloys and pure aluminium, i.e. 11% Si > 7% Si > 22% Si > pure aluminium. Values of $R \times 10^2$ in 0.5 N H_3PO_4 for this order are 1, 0.829, 0.450 and 0.117 (ml cm^{-2} min^{-1}) while R' x 10^5 values were 0.732, 0.674, 0.389 and 0.101 (g cm^{-2} min^{-1}).

The dissolution of aluminium in H_3PO_4 was considered in view of the values of the three step dissociation constants of H_3PO_4. The possible reactions with dissociated H_3PO_4 proceeds as follows:

$$Al^{3+} + 3H_2PO_4^- \longrightarrow Al(H_2PO_4)_3 \qquad (4)$$

$$\text{or } Al^{3+} + 3HPO_4^{2-} \longrightarrow Al_2(HPO_4)_3 \qquad (5)$$

Practically PO_4^{2-} ions do not exist in the solution initially, as the value of the dissociation constant of this step is extremely low. Since $Al_2(HPO_4)_3$ is less soluble than $Al(H_2PO_4)_3$, the corrosion of aluminium proceeds thus [23].

$$Al + 3H_3PO_4 \longrightarrow Al(H_2PO_4)_3 + \frac{3}{2}H_2 \qquad (6)$$

Organic acid media

The polarization behaviour of the alloys was studied in three organic acid media, namely oxalic, tartaric and succinic acids in the concentration range 10^{-1} to 2 N. There is a systematic increase in cathodic and anodic currents for all alloys in the presence of any of the three acids as the acid concentration increases. Limiting values of the current were reached on anodic polarization at potentials which became progressively more positive as the acid concentration increased.

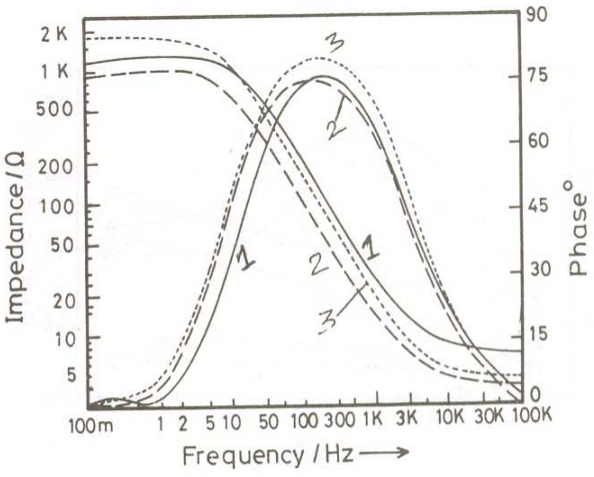

Fig. 6: Bode plot for the alloys in 0.5 N H_2SO_4
(1) 7% Si (2) 11% Si (3) 22% Si

TABLE II: Variation of R_p (K Ω cm^2) for the alloys with organic acid concentration

C	Oxalic acid			Tartaric acid			Succinic acid		
(N)	7% Si	11% Si	22% Si	7% Si	11% Si	22% Si	7% Si	11% Si	22% Si
0.10	0.978	0.673	1.401	25.36	24.53	41.10	90.92	86.83	96.73
0.25	0.422	0.439	0.821	21.51	14.93	22.08	68.97	46.37	88.33
0.50	0.359	0.331	0.449	19.22	14.59	19.36	60.07	58.70	70.06
1.00	0.342	0.291	0.378	—	13.94	—	53.53	39.68	50.77
2.00	0.336	0.259	0.331	15.99	9.64	16.05	—	—	—

In general, low corrosion in these acids is reflected in the low i_{corr} and high R_p values (Table II), if compared with the values obtained in inorganic acids. The exception is oxalic acid, where i_{corr} values are higher than in H_2SO_4. For one and the same alloy, i_{corr} values decrease in the order oxalic > tartaric > succinic acid, at the same acid concentration. This is the same order of K_a values [24] indicating that as a first approximation, corrosion increases with availability of H^+ ions. A similar observation on the relation of corrosion rates with K_a values of organic acids were reported [25].

The polarization behaviour of the alloys was compared with that of pure aluminium in each acid, at a concentration of 0.5 N. For all alloys and aluminium, values of i_1 are higher in oxalic than tartaric or succinic acids. In all cases, the highest i_{corr} values were those recorded for 11% Si. From i_{corr} values, the order of corrosion susceptibility obtained was 11% Si > 7% Si > 22% Si > pure aluminium as in inorganic acids. When aluminium metal is submitted to high positive potentials, a porous oxide layer of significant thickness and regular structure is formed which, in presence of sulphate or oxalate anions, undergoes some anodic dissolution [25]. The outer porous layer was shown to be formed of two zones, the outer zone in contact with the solution incorporates the anions from the solution and has a higher rate of dissolution. This outer layer covers the inner thin barrier layer which resists dissolution [26]. The low corrosion rates observed in case of succinic and tartaric acids are related to formation of the high resistance anodic films in these media and therefore their low solubilities.

Alkaline medium

Studies in NaOH were carried out by polarization, chemical and EIS measurements. It is well known that corrosion of aluminium is relatively higher in alkaline than acid media [27]. The metal undergoes violent corrosion according to [28].

$$Al + OH^- + H_2O \longrightarrow AlO_2^- + \frac{3}{2}H_2 \qquad (7)$$

Polarization measurements of the three alloys as function of NaOH concentration, which was limited by the previous considerations, was carried out, Fig. 7. A major difference as compared with acid media is the shift of OCP to more negative values with concentration. During corrosion of aluminium in alkaline solutions the metal establishes very negative potentials [12,29]. On anodic polarization and at high current density

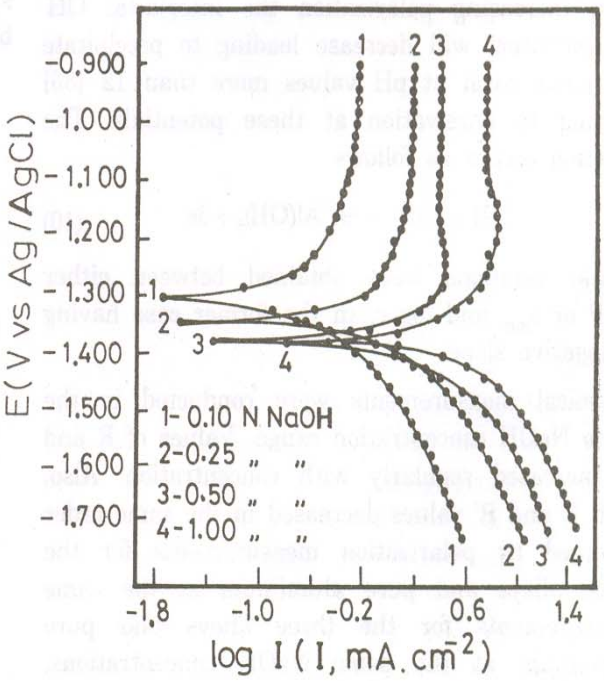

Fig. 7: Polarization curves for the alloy 7% Si as function of NaOH concentration

values there is deviation from the Tafel relation with appearance of limiting currents which increase with NaOH concentration, in accordance with the proportionality reported between i_1 and pH observed during anodic dissolution of aluminium [30].

Since the current in the anodic region increases with NaOH concentration (increase in pH) OH^- ions are assumed to participate in the anodic process. The anodic reaction in the potential region less positive than that at which i_1 appears, leads to formation of AlO_2^- or $Al(OH)_4^-$ (which is equivalent to AlO_2^- [31] by

$$Al + 4OH^- \longrightarrow AlO_2^- + 2H_2O + 3e \quad (8)$$

$$\text{or } Al + 4OH^- \longrightarrow Al(OH)_4^- + 3e \quad (9)$$

Both AlO_2^- and $Al(OH)_4^-$ are soluble products. The slow step in the anodic reaction is either formation of $Al(OH)_4^-$ or its transfer from the surface to the bulk of solution. A change in the diffusion layer thickness at the electrode will cause the anodic current to increase if the mass transfer is the slow step [32]. It is apparent, therefore, that mass transfer of $Al(OH)_4^-$ is the slow step at potentials less positive than i_1.

At high concentrations, a small hump is detected which is associated with formation of an insoluble product, probably $Al(OH)_3$. At these potentials and with increasing polarization the interfacial OH^- concentration will decrease leading to precipitate formation even at pH values more than 12 [33] leading to passivation at these potentials. The reaction occurs as follows

$$Al + 3OH^- \longrightarrow Al(OH)_3 + 3e \quad (10)$$

Linear relations were obtained between either OCP or i_{corr} and log c, in the former case having a negative slope.

Chemical measurements were conducted in the same NaOH concentration range. Values of R and R' increased regularly with concentration. Also, both R and R' values decreased in the same order obtained by polarization measurements for the three alloys and pure aluminium at the same measurements for the three alloys and pure aluminium at the same NaOH concentrations, showing that alloy II has the lowest corrosion resistance, while pure aluminium has the highest.

An observation, however, was made that at low NaOH concentrations and on prolonged immersion times the corrosion rate slows down. On initial immersion, aluminium dissolution proceeds at flaw sites or at more cathodic phases. The OH^- ions penetrate the air formed film, causing dissolution and desaggregation behind the penetration front. This assists outward ionic migration of the mobile Al^{3+} ions and inward mobile O^{2-} ions [34]. The outward mobile Al^{3+} ions will be ejected directly into the solution without assisting in film formation. On prolonged immersion the outer film undergoes aging phenomena which leads to a reduction of porosity in the initially formed film or at the surface of the inner film. This leads to blocking of solution access to the metal/film surface and decrease in corrosion rate [27].

EIS measurements in aerated 10^{-2} N NaOH solutions were carried out on the three alloys after 60 minutes immersion. The Bode plot is shown in Fig. 8. The log Z relation for any alloy develops a number of plateaus over the frequency range studied, indicating different time constants. This may be connected with the stepwise addition of OH^- ions that has been reported during formation of $Al(OH)_4^-$ [35]. The absence of linear log Z relations with a slope of -1 and the departure of θ_{max} at intermediate frequencies from 90^0 which is expected in case of purely capacitive behaviour shows that the circuit tends to the resistive behaviour.

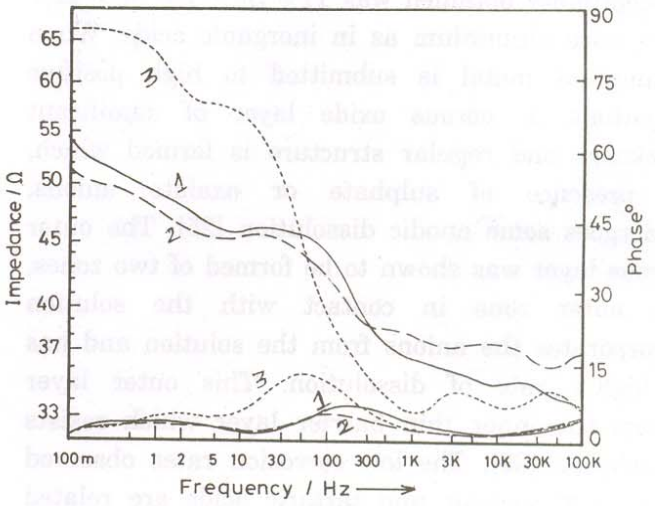

Fig. 8: Bode plots for the three alloys in 10^{-2} N NaOH
(1) 7% Si (2) 11% Si (3) 22% Si

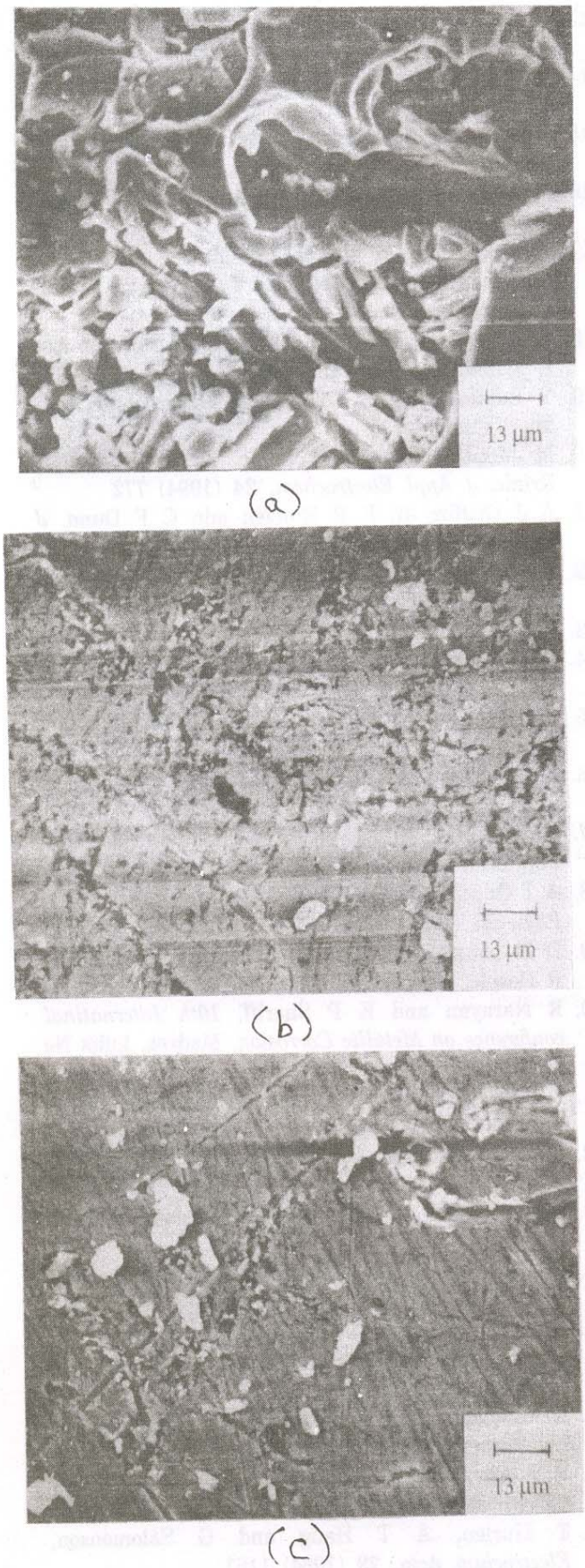

Fig. 9: Micrographs for alloy 11% Si after immersion in (a) 10^{-2} N NaOH: severe corrosion of all types (b) 3 N H_2SO_4: weak general corrosion and (c) 2 N oxalic acid: weak general corrosion (White spots in (b) and (c) are corrosion products)

Even under severe conditions of corrosion observed in NaOH, there is still consistency in values of the impedance, Z at low frequencies with those observed in H_2SO_4, i.e. Z for the alloys follows the order 22% Si > 7% Si > 11% Si. θ_{max} for the alloys are in the same order. These results confirm that as in acid media, alloy 11% Si corrodes more than the other two alloys in alkaline media.

Scanning electron micrography

Fig. 9 shows micrographs of alloy 11% Si after 60 minutes immersion in different solutions. This alloy is mainly formed of the eutectic. The points of high stress are in the eutectic net which is the region where attack initiates. When subjected to a highly corrosive medium (10^{-2} N NaOH) severe corrosion of all types was apparent, while in less corrosive media (3 N H_2SO_4 or 2 N oxalic acid) the mild attack produced weak general corrosion.

General remarks

The results of EIS, polarization and chemical measurements have indicated that the alloys 7% Si and 22% Si have better corrosion resistance than alloy 11% Si. This is probably due to the stabilization of the oxide film by incorporation of elemental aluminium (in case of alloy 7% Si) or Si (in case of alloy 22% Si) [36].

The difference in corrosion rates obtained in presence of different anions is explained by the chemical nature of the corrosion reaction which involves metal anion species which direct the breakdown or formation of a protective reaction product on the surface [8,37]. The difference in corrosion rates obtained for a certain alloy in acid media in presence of the different anions is due to the difference in the bonding strength of these ions on different sites on the surface. The higher rates of corrosion observed in NaOH are due to the decrease in thickness of the thin inner barrier layer covering aluminium when the pH is increased [38]. this layer is responsible for protecting the metal from corrosion and as it becomes thinner, attack by NaOH is facilitated, since the outer layer is of the non barrier type.

CONCLUSION

- Aluminium-silicon alloys corrode in aqueous media more than pure aluminium. Presence of elemental silicon or aluminium probably causes

stabilization of oxide films on alloys 22% Si or 7% Si, respectively, as compared to alloy 11% Si, which is formed nearly completely of the eutectic.

- The corrosion rate for any alloy in the media investigated decreases in the order NaOH > H_3PO_4 > H_2SO_4 > oxalic acid > tartaric acid > succinic acid.
- Corrosion rates in organic acids fall with decrease in their K_a values. However, a detailed study of the adsorption of the anions on the surface film or their incorporation therein is required to clarify the role of organic anions in the corrosion process.
- Capacitive behaviour controls the circuit in H_2SO_4 medium, in contrast to resistive control in NaOH medium.

Acknowledgement: A A Mazhar thanks the Alexander Von Humboldt Foundation for providing the equipment used in EIS measurements.

REFERENCES

1. H S Wroblowa, in B E Conway and J O M Bockris (Eds), *Batteries for vehicular propulsion, Modern Aspects of Electrochemistry,* Plenum, New York (1985) 371
2. E Deltombe, C Vanleugenhaghe and M Pourbaix, *Atlas of Electrochemical Equilibria in Aqueous solutions,* NACE, Houston, Texas (1974) 168
3. G Bombara and U Bernabai, *Brit Corros J,* **11(1)** (1976) 25
4. J L Murray and A J McAlister, *Bull of Alloy Phase Diagrams,* **5(1)** (1984) 74
5. P Carbonini, T Monetta, D B Milton, F Bellucci, P Mastronardi and B Scatteia, *J Appl Electrochem,* **27(10)** (1997) 1135
6. A Conde and J de Damborenea, *Electrochim Acta,* **43(8)** (1998) 849
7. S Kuroda and K Tohma, *J Jap Inst of Light Metals,* **48(6)** (1998) 282
8. R T Foley, *J Electrochem Soc,* **122** (1975) 1493
9. B Muller, K Franze and D Mebarek, **51(8)** (1995) 625
10. M Elboujdaini and E Ghali, *Corros Sci,* **30(8-9)** (1990) 855
11. F Holzer, S Müller, J Desilvestro and O Haas, *J Appl Electrochem,* **23** (1993) 125
12. J F Cooper, Weight and Volume estimates for aluminium-air batteries designed for electric vehicle application, p 81, *Proc First International Workshop on Reactive Metal-Air batteries,* Universtiy of Bonn (1979)
13. F M Al-Kharafi and W A Badawy, *Electrochim Acta,* **40(12)** (1995) 1811
14. J Radosevic and M Kliskic, *J Appl Electrochem,* **22** (1992) 189
15. J W Diggle, T C Downie and C W Goulding, *Chem Rev,* **65** (1969) 365
16. K S N Murthy and E S Dwarakadasa, *Brit Corros J,* **30(2)** (1995) 111
17. H Takahashi, M Mukai and M Nagayama, *Proc 9th Int Congress Met Corrosion, toronto,* (June 1984) Vol 2, 155
18. L Tomcsanyi, K Varga, I Bartik, G Horanyi and E Maleczki, *Electrochim Acta,* **34(6)** (1989) 855
19. Y Fukuda and T Fukushima, *Electrochim Acta,* **28(1)** (1983) 47
20. M Metikos-Hukovic, R Babic, Z Grubac and S Brinic, *J Appl Electrochem,* **24** (1994) 772
21. A J Griffin, Jf, F R Brotzen adn C F Dunn, *J Electrochem Soc,* **141(2)** (1994) 3473
22. F Mansfeld, M W Kendig and S Tsai, *Corrosion,* **38** (1982) 570
23. R S Dubey, *Bull Electrochem,* **12(7-8)** (1996) 467
24. R C Weast (Ed), *Handbook of Chemistry and Physics,* 67th edn, CRC Press, Florida (1987)
25. K Sakigawa and M Kobiyama, *J Jap Inst of Light Metals,* **42(4)** (1992) 205
26. A A Mazhar, F El Taib Heakal and A S Mogoda, *Corrosion,* **44(6)** (1988) 322
27. M R Tabrizi, S B Lyon, G E Thompson and J M Ferguson, *Corros Sci,* **32(7)** (1991) 733
28. A I Onuchukwu and A A I Adamu, *Mater Chem Phys,* **25** (1990) 227
29. D M Drazic, S K Zecevic, R T Atanasoski and A R Despic, *Electrochim Acta,* **28(5)** (1983) 751
30. R Narayan and K P Sheriff, *10th Internatinal conference on Metallic Corrosion,* Madras, India No v. (1987)
31. C B Breslin, L P Friery and W M Carroll, *Corros Sci,* **36(1)** (1994) 85
32. R D Armstrong and V J Braham, *Corros Sci,* **38(9)** (1996) 1463
33. C M Rangel and M Travassos, *Corros Sci,* **33** (1992) 327
34. R S Alwitt, *Oxides and Oxide Films,* 4 M Dekker, New York (1976)
35. D D Macdonald, S Real, S I Smedley and M Urquidi - Macdonald, *J Electrochem Soc,* **135** (1988) 2410
36. R Ambat and E S Dwarakadasa, *J Appl Electrochem,* **24** (1994) 911
37. R T Foley and P P Trzaskoma, *Corrosion, NACE,* **33(12)** (1977) 435
38. T Hurlen, A T Haug and G Salomonson, *Electrochim Acta,* **29** (1984) 1161